An Improved Nonparametric Method for Fault Detection of Induction Motors Based on the Statistics of the Fractional Moments

Arsenii L Morozov[1], Raoul R Nigmatullin[1], Paolo Lino[2], Guido Maione[2], Silvio Stasi[2]

Abstract— **Accurate detection of faults of induction motors is an important challenge for industry. Often only stator currents/voltages are measurable and, hence, can be analyzed for fault detection. Among current analysis methods, the most attractive ones have low computational cost and little memory requirement for treatment of the measured data. Motor current signature analysis based on Fast Fourier Transform (FFT) provides fast computation, however it requires a long acquisition time interval for accurate fault detection. In fact, a short acquisition time causes the available frequency resolution of FFT spectrum to decrease and, hence, the spectra of the healthy and broken motors become indistinguishable. Recently, a statistical method, the so-called Statistics of Fractional Moments (SFM) allowed to distinguish signals with small differences. The statistically "close" signals are clustered and separated from "anomalous" signals. In this paper, the FFT and SFM are combined to reduce the acquisition time interval and hence the required memory and computation, while the fault detection capability is preserved. The effectiveness of the proposed approach is tested both on a healthy induction motor and on the same motor with broken rotor bars, for different acquisition time intervals.**

I. INTRODUCTION

Induction motors (IM) are widely used in industry due to their reliability, low cost, fast speed, high overload capability and high efficiency [1]–[8]. Different kinds of fault, which are difficult to detect, can reduce IM efficiency and performance and hence increase energy consumption and long-term degradation. Then it is extremely important to detect and identify faults as early as possible.

In this paper, detection means determining the motor condition, i.e. "healthy" or "faulty". Main faults in IM include the following [1], [2]:

1) Stator faults (winding open-phase or short-circuit of a few turns in a phase winding).
2) Rotor electrical faults (rotor winding open-phase for wound rotor machines and broken bar(s) or cracked end-ring for squirrel-cage machines).
3) Rotor mechanical faults (bearing damage, eccentricity, bent shaft, axis misalignment).
4) Failure of one or more power electronic components of the drive system.

Although rotor faults are about 10% of all possible faults, in such conditions the motor operation is not restricted and can determine further faults and malfunctions [2]. For this reason, many researches developed and tested methods able to recognize this specific kind of faults. Fault detection methods generally can be invasive or non-invasive. Invasive methods monitor main parameters of motors like asymmetrical magnetic flux distribution [9], vibration [10], acoustic emission, temperature, oil or debris analysis [11], [12]. They require additional sensors and costly measurement equipment (e.g. vibration or torque sensors, etc.). Non-invasive methods are based on measurement of electrical variables, like stator-phase voltages and currents. They are more interesting, mainly because their cost is acceptable and they do not require direct access to internal motor parts. They are based on the evidence that three-phase stator currents are affected by eccentricity between stator and rotor, torque oscillations, disturbance in electro-magnetic forces that are caused by faults. These influences lead to the appearance of additional frequencies in the current spectrum. In [2], the relationship between the type of faults and the occurrence of harmonics in the currents spectrum is derived. A detailed quantitative analysis of the effect of faults on the currents spectrum is presented in [2], [3] and references therein.

Non-invasive techniques that process stator currents are usually classified as: frequency-domain, time-domain and time-frequency domain. The choice of a signal processing technique depends on IM working conditions. A nonstationary condition indicates variable motor speed, for which time-domain and time-frequency domain analysis are employed. In stationary conditions, the rotor speed is nearly constant in the considered period. In this paper, the focus is on fault detection of IM in stationary conditions.

Spectral estimation techniques are usually applied in stationary conditions for monitoring and detection. They imply accurate tracking of harmonic components associated with the considered faults and caused by different phenomena. The separation of harmonic components related to the important frequencies requires a high frequency resolution. High-resolution methods such as Multiple SIgnal Classification [13], [14] and Estimation of Signal Parameters via Rotational Invariance Techniques [3], [15] allow to reduce the acquisition time interval but they are rather complex to use in real time. Fast Fourier Transform (FFT) is commonly used, but it takes a very long acquisition time interval to obtain an acceptable frequency resolution, which is inversely proportional to such interval. The zoom-FFT (ZFFT) considers only a short frequency bandwidth for accurate fault detection [16]–[18]. This technique can reduce the computational time, and hence the required memory, and increase the accuracy

[1]A. L. Morozov and R. R. Nigmatullin are with Radioelectronic and Informative-Measurement Technics Department, Kazan National Research Technical University named after A. N. Tupolev - Kazan Aviation Institute, Kazan, Tatarstan 420010, Russian Fed. {morozovars@yandex.ru, renigmat@gmail.com}

[2]P. Lino, G. Maione and S. Stasi are with the Department of Electrical and Information Engineering, Polytechnic University of Bari, Bari, 70125, Italy {paolo.lino,guido.maione,silvio.stasi}@poliba.it

in a specified frequency range. But ZFFT is affected by the selection of the proper acquisition time interval.

Recently, a new statistical method, named the Statistics of Fractional Moments (SFM), was developed to distinguish signals with low signal-to-noise ratio [19]. Signals are transformed in the space of fractional moments, where they can be distinguished and clusterized. The SFM is extremely sensitive to very small differences between signals. It allows to present and describe any random sequence of data in the moments space [19], [20]. Since the GMV (generalized mean value) function can be approximated by a linear combination of exponential functions, the random sequences can be expressed in terms of a reduced number of parameters (much lower than the number of data). This representation is convenient for comparing different sequences.

In this paper, the SFM method is applied to FFT spectra (FFT+SFM) to reduce the required acquisition time interval for faults detection in IM working in stationary conditions. This approach combines the good computational efficiency of the FFT and the resolution improvement achieved by the SFM to realize a fast and accurate fault detection. The effectiveness of the proposed approach is evaluated by processing measurement data of a healthy motor and a motor with one broken bar in stationary conditions, with different acquisition time intervals. To prove the reliability and reproducibility of the results with short acquisition time intervals, tests are repeated for a number of similar measurement acquisitions. This number grows while the acquisition time decreases. Hence the approach helps fault detection. Moreover, some parameters can be used as fault indicators because they do not depend on the acquisition time interval. The fault detection results in this paper are obtained by analyzing data in a short acquisition time interval; the same method has been successfully applied to detect other types of faults, like stator faults. To allow fault diagnosis and discriminate one fault from another, a larger time interval could be necessary. Our conjecture is that slope of the moments curve is related to the type of fault.

The paper is structured as follows. The properties of the FFT and SFM methods are described in subsections II-A and II-B, respectively. The algorithm of the FFT+SFM combination is presented in subsection II-C. In section III, the results provided by experimental tests of the FFT+SFM are shown and discussed. Section IV collects conclusions and final remarks.

II. THE FAULT DETECTION METHOD

A. Basics of the Fast Fourier Transform

The FFT algorithm is one of the fastest and most effective way to obtain the frequency spectrum. The accuracy and frequency resolution of the spectrum computed by the FFT depends on the sample frequency and the acquisition time interval. Obviously, the sample frequency should be higher than the highest frequency in the analyzed signal. The number of points or the acquisition time interval influences the resolution. On one hand, a long acquisition time interval allows high resolution, on the other hand, a short acquisition time interval requires less computational time and memory.

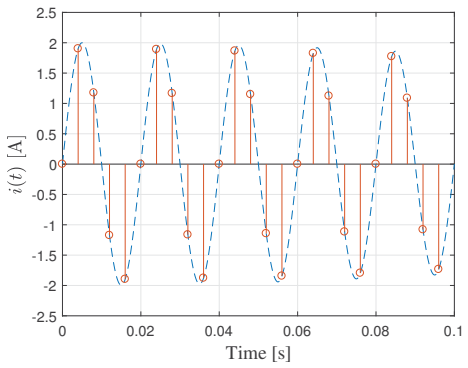

Fig. 1. Signal in (1)

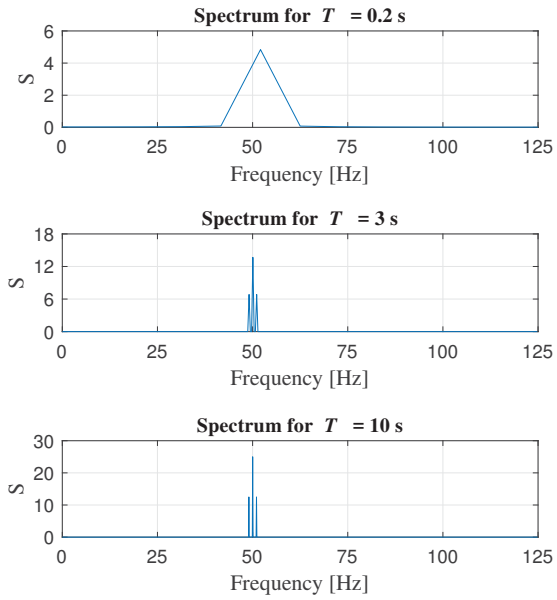

Fig. 2. Spectrum of signal in (1) for different acquisition times T

Let us consider a signal with three sinusoidal components:

$$i(t_i) = \sin(2\pi f_1 t_i) + 0.5\,\sin(2\pi f_2 t_i) + 0.5\,\sin(2\pi f_3 t_i) \quad (1)$$

with $f_1 = 50$ Hertz, $f_2 = 49$ Hertz, $f_3 = 51$ Hertz. The time variable is set as $t_i = i/f_s$, where f_s is the sample frequency, $i = 0, 1, \ldots, N$, $N = f_s T$ is the number of points depending on the chosen acquisition time interval T. Fig. 1 shows the signal (1) after sampling at $f_s = 250$ Hertz, while Fig. 2 shows the spectrum amplitude S obtained by FFT for different values of T, i.e. 0.2, 3 and 10 seconds. When $T = 10$ seconds, FFT is able to distinguish the harmonic components. However, for $T = 3$ and 0.2 seconds, it becomes impossible to distinguish the different components, although the last case is preferable because it demands less memory and faster computations. Namely,

the number of output points after the application of the FFT equals the number of input points N. Therefore, the frequency resolution is equal to:

$$\Delta f = \frac{f_s}{N} = \frac{f_s}{f_s T} = \frac{1}{T}. \tag{2}$$

Then, one can conclude that a very long acquisition time interval is needed for a good frequency resolution of the FFT. With a poor frequency resolution, the significant information about the harmonic components induced by faults can be hidden by the spectral leakage. Then the simple FFT can not be used in this case. Moreover, the fault detection method should have a low sensitivity to the measurement noise.

B. Basics of the Statistics of the Fractional Moments

Fault detection in very short acquisition time has not been deeply tackled and solved, as far as the authors know. Now it can be approached by deep statistical analysis of the "poor" frequency resolution that is present in the FFT spectra. To this aim, the recent SFM method can be considered. It extends the integer moments, by assuming fractional values of the moments' order. Further details are in [19]. The value of the moment having a mom_p order for the input random sequence $y_1, y_2, \ldots, y_N$ is defined by:

$$\Delta_N^{(mom_p)} = \sum_{i=1}^{N} |y_i|^{mom_p} \tag{3}$$

where, in this study, the input sequence is given by the amplitudes in the stator current spectrum. To limit the increase of $\Delta_N^{(mom_p)}$ with the moment's order mom_p, the random sequence can be preliminarily normalized as follows:

$$nrm_i = \frac{|y_i|}{\|y\|_\infty} \tag{4}$$

where nrm_i $(i = 1, 2, \ldots, N)$ is the normalized sequence and $\|y\|_\infty = \max\{|y_1|, |y_2|, \ldots, |y_N|\}$. Note that the proposed fault detection method requires the time needed to acquire data and the computation time. These operations can be iteratively repeated during motor operation, and sliding time windows can be used to perform an almost continuous monitoring and detection of faults. Anyway, on the contrary, most of spectral estimation techniques are off-line. Here, modulus is used because y_i are complex numbers coming from FFT. Hence the input sequence is finally given by the amplitudes in the stator current spectrum. The normalized sequence is located in the interval $0 < nrm_i < 1$. Therefore, the normalized moment with mom_p order is:

$$\overline{\Delta}_N^{(mom_p)} = \sum_{i=1}^{N} nrm_i^{mom_p} = \sum_{i=1}^{N} \left(\frac{|y_i|}{\|y\|_\infty} \right)^{mom_p} \tag{5}$$

If $mom_p \to 0$, $\overline{\Delta}_N^{(mom_p)}$ coincides with the number of data points N; if $mom_p \to \infty$, $\overline{\Delta}_N^{(mom_p)}$ tends to zero.

The set of orders that are necessary and sufficient (other orders give a negligible contribution) to detect differences between the considered sequences are computed as [21]:

$$mom_p = \exp\left\{ min + \frac{p}{P} (max - min) \right\} \tag{6}$$

where $p = 0, 1, \ldots, P$, min and max define the limits in the logarithmic scale, P is the resolution factor for the moments order. For this specific application, the values of $min = -15$ and $max = 15$ are determined by experiments. They allow to obtain the full shape of the moments curve that results from (5), because a saturation phenomenon takes place at the left and right sides of the curve. Lower min and max values don't change the shape of the curve. Usually, the resolution factor creating the correct number of the discrete moments is located in the interval $50 \leq P \leq 100$ [21].

This simple transformation allows to represent any random sequence by a monotonically increasing curve in the space of moments. Then, to compare different sequences, one should find an aggregated parameter that can quantify the difference. As shown below, this parameter can be given by the slope of the so-called moments curve. The last is the plot of the healthy/faulty motor's moments against the moments of a healthy motor, taken as reference. Slopes are calculated by the Linear Least Square Method (LLSM). If the slope is 1, then the two compared sequences show the minimal difference, while different slopes exhibit a quantitative difference between the compared sequences.

C. Data Analysis based on Fast Fourier Transform and Statistics of Fractional Moments

The procedure consists of three simple operations that must be successively applied to the stator three-phase currents for detecting the faults. The first two are usually employed by the approach named Motor Current Signature Analysis. The third step improves the fault detection capability in case of poor frequency resolution.

- Step 1: $\alpha - \beta$ coordinates transformation. The three-phase stator currents of IM can be represented as a rotating space vector in a complex reference frame attached to the stator phase plane. The real axis α is aligned to the axis of one stator winding (for example phase u), while the imaginary axis β is phase shifted of 90 electrical degrees. The coordinate transformation from phase currents u, v, w to the α, β ones (the zero sequence current $i_0 = 0$ because of the windings connection) is obtained by the following matrix operation:

$$\begin{bmatrix} i_\alpha \\ i_\beta \end{bmatrix} = \frac{2}{3} \begin{bmatrix} 1 & -1/2 & -1/2 \\ 0 & \sqrt{3}/2 & -\sqrt{3}/2 \end{bmatrix} \begin{bmatrix} i_u \\ i_v \\ i_w \end{bmatrix} \tag{7}$$

  Sampling the current space vector (i.e. the real and imaginary components) leads to a complex sequence.
- Step 2: Complex FFT computation. A complex FFT is applied to derive the amplitude-frequency response from the complex sequence from the previous step.
- Step 3: SFM computation. The obtained sequence spectrum is normalized by (4). Then, the set of moments' orders and the moments sequences for the spectrum of Step 2 are computed by (6) and (5), respectively. Finally, the slopes are calculated by the LLSM.

The pattern sequence is obviously given by a healthy motor, which is working in the same load condition as the

other tested motors. Then, the calculated slopes can be used as fault indicators. If a slope is equal or very close to 1, then the tested motor is healthy. A significant deviation from 1 implies that the spectrum of the tested motor contains some harmonic components that may be caused by faults.

Note also that the moments curves are sensitive to the number of points contained in the input sequences. In the proposed approach, the input sequence coincides with the FFT spectrum. The number of points in the FFT spectrum depends on the sample frequency and the acquisition time interval. Then, the slopes should be calculated and compared for measurements that were obtained by the same sample frequency and acquisition time interval. To summarize, the fault detection approach is based on the slopes of the moments curves for healthy and broken motors, respectively. This information should be taken into account when testing or monitoring motors.

III. INDUCTION MACHINE FAULT DETECTION

A. Experimental Set-up

A set of experiments has been performed for testing the proposed fault detection method on two 1.1 kW IM, a healthy one and a faulty one with a broken rotor bar. The motors have an input voltage of 380 V, a supply frequency of 50 Hertz, a 100% load. The three-phase stator currents have been measured and stored by a Teledyne Lecroy HDO 6034 oscilloscope. A sampling frequency of 1000 Hertz has been used for data acquisition. Different acquisition time intervals have been considered: 50 s, 20 s, 10 s, 1 s, 0.5 s, 0.2 s. Moreover, it is important to guarantee that the results always give the same indication (the fault) in the same experimental condition (acquisition time interval). To this aim, for different time intervals, the measurements for short acquisition time intervals have been repeated as follows ($\{$*Acquisition time interval* $[s]$, *Number of repetitions*$\}$): $\{50, 1\}$; $\{20, 4\}$; $\{10, 8\}$; $\{1, 80\}$; $\{0.5, 160\}$; $\{0.2, 400\}$. The shorter is the acquisition interval, the more repetitions are required.

B. Experimental Results

All steps of the proposed method are now presented. Fig. 3 (a) shows the measured one-phase stator current for the healthy motor and for the faulty motor, respectively. The first step is the transformation from three-phase coordinates to $\alpha - \beta$ components in the complex stator reference-frame. Fig. 3 (b)-(c) show the $\alpha - \beta$ stator current components for the healthy and faulty motor. The second step is based on the application of the FFT. Fig. 4 (a)–(f) show the obtained FFT spectra for different acquisition time intervals, i.e. 50 s, 20 s, 10 s, 1 s, 0.5 s, 0.2 s, respectively. Blue lines represent the spectrum obtained for the healthy motor, red lines the spectrum for the faulty motor. Sideband harmonic components in the spectrum of the broken motor are fault indicators, for FFT. On the plots, where detection is possible, i.e. in cases (a)–(c), the corresponding sideband harmonic components are tagged. The FFT analysis becomes useless with short acquisition time intervals (lower than 10 s), see cases (d)–(f).

The normalized moments $\overline{\Delta}$ for each spectrum, as obtained in the previous step, are computed by (5). For calculation of $\overline{\Delta}$, the set of moments orders are obtained by (6). The values of $\overline{\Delta}$ for every spectrum are shown in Fig. 5: the blue curves refer to the healthy motor, the red curves mark the broken motor. Obviously, the values of $\overline{\Delta}$ that are obtained for different acquisition time intervals cannot be compared with each other, whereas the moments to be compared are computed in the same acquisition time interval.

It is instructive to present the differences of $\overline{\Delta}$ obtained for the healthy and faulty motors by the slopes of the moment curves. The differences can be clearly seen on the graph of the obtained moments $\overline{\Delta}$ for each tested motor against the $\overline{\Delta}$ for the healthy motor. The plots for an acquisition time interval of 50 s and 0.2 s are shown in Fig. 6 (a)-(b), respectively. The obtained plots demonstrate the following important fact: the combination FFT+SFM allows to diminish the lower limits for the short acquisition intervals, while keeping the possibility of long acquisition intervals, and save the fault detection capability.

The values of the slopes can be used as fault indicator. To evaluate the invariance of this parameter, measurements for short acquisition time intervals have been repeated as previously specified. The moments sequence obtained by the first of the 400 measurements for $T = 0.2$ seconds on the healthy motor has been chosen as the pattern one. Then the desired slopes corresponding to the healthy motor and the slopes of the faulty motor were calculated by LLSM. This operation has been repeated for every considered acquisition time interval. The average values and standard deviations of the slope for every acquisition interval are given in Table I.

The variations of the obtained slopes caused by random fluctuations for different measurements and for $T = 0.2$ seconds are shown in Fig. 7. The blue line corresponds to the slopes obtained for the healthy motor, while the red line corresponds to the values obtained for the motor with one broken rotor bar.

IV. CONCLUSIONS

The reduction of the required acquisition time interval, when the fault is still detectable, is an important challenge for induction machines. A short acquisition time interval allows overcoming the economic problems related to the usage of expensive equipment for measurements and computation.

The combination of the FFT and SFM methods allow to reduce the acquisition time interval in experiments for fault detection. The proposed approach demonstrates its effectiveness for one broken rotor bar in relatively short acquisition time intervals, i.e. 0.2 s. The invariance of this result has been proved statistically by a large number of measurements, as Fig. 7 and Table I show.

Detection of different faults by the proposed combination FFT+SFM will be considered to test the diagnostic properties of the method. Moreover, some equipment could be developed for analysis of the three-phase stator currents

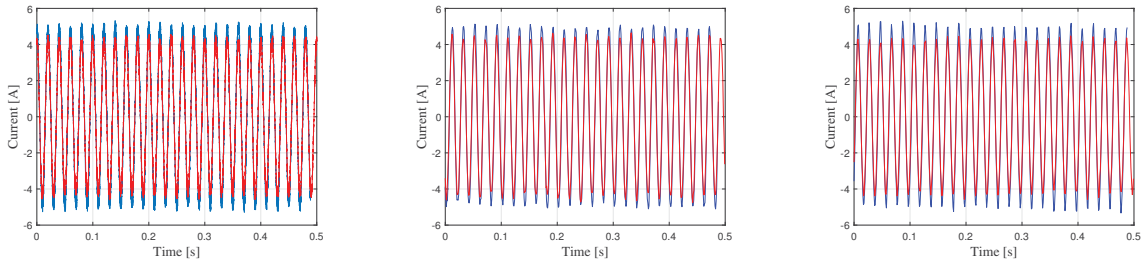

(a) Measured one-phase current (b) α component (c) β component

Fig. 3. Measured currents for a healthy motor (blue line) and a faulty motor (red line) with one broken rotor bar

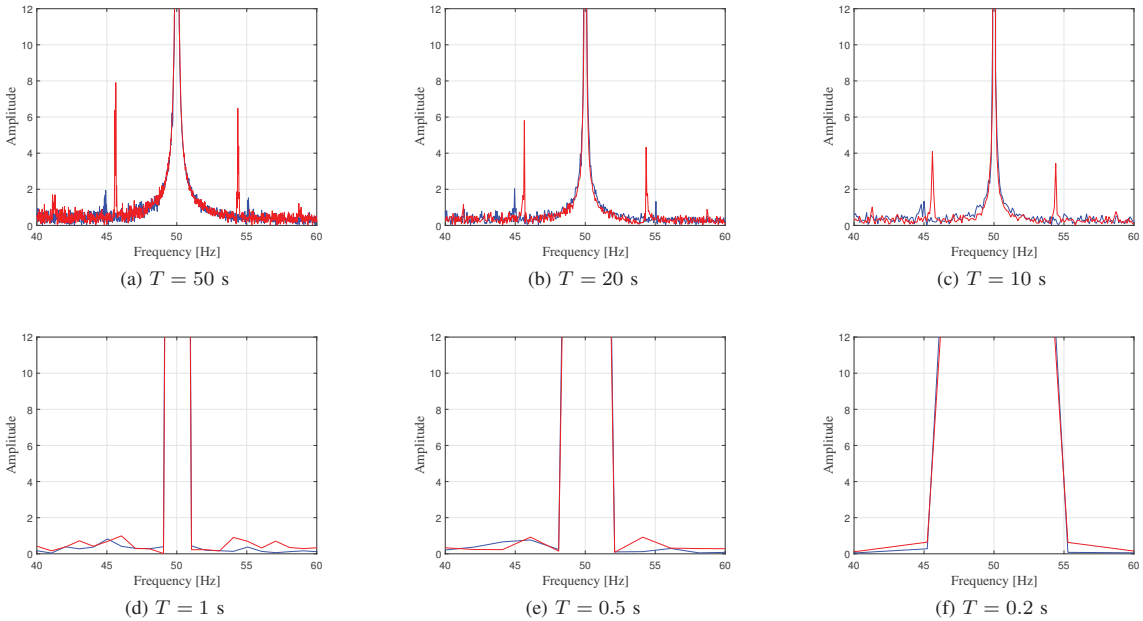

(a) $T = 50$ s (b) $T = 20$ s (c) $T = 10$ s

(d) $T = 1$ s (e) $T = 0.5$ s (f) $T = 0.2$ s

Fig. 4. FFT spectra for different acquisition time intervals T

TABLE I

STATISTICAL PARAMETERS OF THE SLOPES

Acquisition time interval [s]	Number of repetitions	Healthy motor			Faulty motor		
		Average	Standard deviation	Max deviation	Average	Standard deviation	Max deviation
50	1	1	—	—	0.875	—	—
20	4	0.998	$6.431 \cdot 10^{-4}$	$1.194 \cdot 10^{-3}$	0.873	$3.218 \cdot 10^{-4}$	$1.182 \cdot 10^{-3}$
10	8	0.998	$1.082 \cdot 10^{-3}$	$2.129 \cdot 10^{-3}$	0.873	$6.292 \cdot 10^{-3}$	$1.672 \cdot 10^{-3}$
1	80	0.996	$3.960 \cdot 10^{-3}$	0.011	0.871	$1.671 \cdot 10^{-3}$	$4.042 \cdot 10^{-3}$
0.5	160	0.996	$4.224 \cdot 10^{-3}$	0.012	0.871	$1.878 \cdot 10^{-3}$	$4.657 \cdot 10^{-3}$
0.2	400	0.995	$4.576 \cdot 10^{-3}$	0.015	0.870	$2.585 \cdot 10^{-3}$	$8.131 \cdot 10^{-3}$

by FFT+SFM. The proposed combination allows to change the acquisition time interval and satisfy low computational requirements that lead to a low price of this equipment.

ACKNOWLEDGMENT

The authors deeply thank Prof. Zoran Jeličić (University of Novi Sad, Serbia) for providing data used in this paper.

REFERENCES

[1] W. T. Thomson and M. Fenger, Current signature analysis to detect induction motor faults, IEEE Industry Applications Magazine, vol. 7, no. 4, pp. 26–34, July/Aug. 2001.

[2] A. Bellini, F. Filippetti, C. Tassoni, and G. A. Capolino, Advances in diagnostic techniques for induction machines, IEEE Trans. Ind. Electron., vol. 55, no. 12, pp. 4109–4126, Dec. 2008.

[3] E. H. El Bouchikhi, V. Choqueuse, and M. Benbouzid, Induction machine diagnosis using stator current advanced signal processing, Int. Journal on Energy Conversion, vol. 3, no. 3, pp. 76–87, 2015.

[4] E. H. El Bouchikhi, V. Choqueuse, and M. Benbouzid, Induction machine faults detection using stator current parametric spectral estimation, Mechanical Systems and Signal Processing, vol. 52–53, pp. 447–464, Feb. 2015.

[5] J. Faiz and M. Ojaghi, Different indexes for eccentricity fault daignosis in three-phase squirrel-cage induction motors: A review, Mechatronics, vol. 19, no. 1, pp. 2–13, Feb. 2009.

[6] F. Filippetti, A. Bellini, and A. Capolino, Condition monitoring and diagnosis of rotor faults in induction machines: State of art and future perspectives, in Proc. 2013 IEEE Worksh. Electrical Machines Design Control and Diagnosis, Paris, France, 11-12 Mar. 2013, pp. 196–209.

[7] F. Duan and R. Živanović, Induction motor stator faults diagnosis by using parameter estimation algorithms, in Proc. 2013 9th IEEE Int. Symp. Diagnostics for Electric Machines, Power Electronics and Drives, Valencia, Spain, 27-30 Aug. 2013, pp. 274–280.

[8] F. Duan and R. Živanović, Induction motor fault diagnostics using global optimization algorithm, in AUPEC'09, 19th Australasian Universities Power Eng. Conf., Adelaide, Australia, 27-30 Sep. 2009.

[9] R. Fišer and S. Ferkolj, Application of a finite element method to predict damaged induction motor performance, IEEE Trans. Magnetics, vol. 37, no. 5, pp. 3635–3639, Sep. 2001.

[10] A. Sadoughi, M. Ebrahimi, and E. Rezaei, A new approach for induction motor broken bar diagnosis by using vibration spectrum, in SICE-ICASE International Joint Conference 2006, Busan, South Korea, 18-21 Oct. 2006, pp. 4715–4720.

[11] Y. Trachi, E. Elbouchikhi, V. Choqueuse, and M. E. H. Benbouzid, Induction machines fault detection based on subspace spectral estimation, IEEE Trans. Ind. Electron., vol. 63, no. 9, pp. 5641–5651, Sep. 2016.

[12] H. A. Toliyat, S. Nandi, S. Choi, and H. Meshgin-Kelk, Electric Machines: Modeling, Condition Monitoring, and Fault Diagnosis. Boca Raton, FL, USA: CRC Press, Oct. 2012.

[13] F. Cupertino, E. de Vanna, G. Forcella, L. Salvatore, and S. Stasi, Detection of IM broken rotor bars using MUSIC pseudo-spectrum and pattern recognition, in Proc. of IECON '03, The 29th Annual Conf. IEEE Ind. Electron. Society, Roanoke, VA, USA, 2-6 Nov. 2003, pp. 2829–2834.

[14] F. Cupertino, G. Martorana, L. Salvatore, and S. Stasi, Diagnostic startup test to detect induction motor broken bars via short-time MUSIC algorithm applied to current space-vector, in Proc. of EPE 2003, 10th Eur. Conf. Power Electron. & App., Toulouse, France, 2-4 Sep. 2003.

[15] Y.-H. Kim, Y.-W. Youn, D.-H. Hwang, J.-H. Sun, and D.-S. Kang, High-resolution parameter estimation method to identify broken rotor bar faults in induction motors, IEEE Trans. Ind. Electron., vol. 60, no. 9, pp. 4103–4117, Sep. 2013.

[16] A. Bellini, A. Yazidi, F. Filippetti, C. Rossi, and G.-A. Capolino, High frequency resolution techniques for rotor fault detection of induction machines, IEEE Trans. Industrial Electronics, vol. 55, no. 12, pp. 4200–4209, Dec. 2008.

[17] F. Cupertino, E. de Vanna, L. Salvatore, and S. Stasi, Analysis techniques for detection of IM broken rotor bars after supply disconnection, IEEE Transactions on Industry Applications, vol. 40, no. 2, pp. 526–533, Mar./Apr. 2004.

[18] F. Cupertino, E. de Vanna, L. Salvatore, and S. Stasi, Comparison of spectral estimation techniques applied to induction motor broken bars detection, in Proc. of SDEMPED 2003 – 4th IEEE International Symposium on Diagnostics for Electric Machines, Power Electronics and Drives, Atlanta, GA, USA, 24-26 Aug. 2003, pp. 129–134.

[19] R. R. Nigmatullin, The statistics of the fractional moments: Is there any chance to "read quantitatively" any randomness?, Journal of Signal Processing, vol. 86, pp. 2529–2547, 2006.

[20] R. R. Nigmatullin and G. Smith, The generalized mean value function approach: A new statistical tool for the detection of weak signals in spectroscopy, Journal of Physics D: Applied Physics, vol. 38, no. 2, pp. 328–337, 2005.

[21] R. R. Nigmatullin, C. Ceglie, G. Maione, D. Striccoli, Reduced fractional modeling of 3D video streams: the FERMA approach, Nonlinear Dynamics, vol. 80, no. 4, pp. 1869–1882, June 2015.

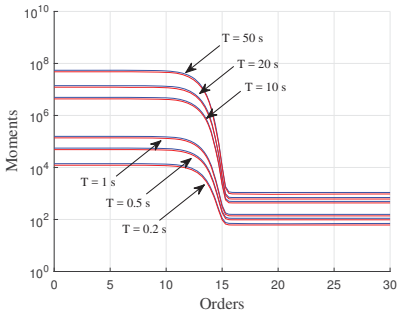

Fig. 5. Moments for different acquisition time intervals T: the blue curves refer to the healthy motor, the red curves to the broken motor

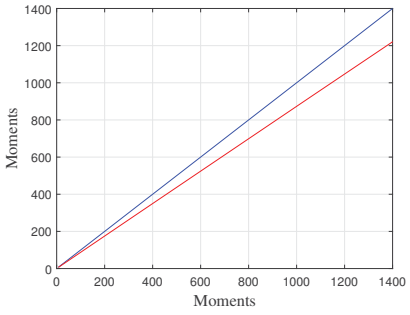

(a) $T = 50$ seconds

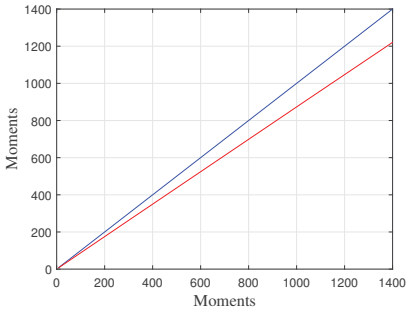

(b) $T = 0.2$ seconds

Fig. 6. Moments of healthy and faulty motor against moments of the healthy motor for two acquisition time intervals: $T = 50$ and 0.2 seconds

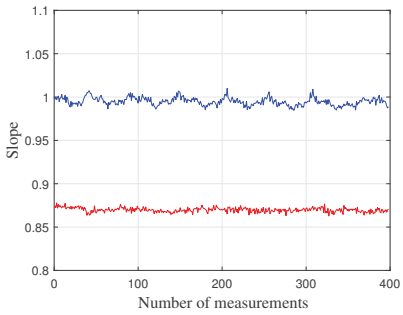

Fig. 7. Dependence of the slopes against number of measurements for acquisition time interval $T = 0.2$ seconds (blue line for healthy motor, red line for motor with one broken rotor bar)